

RESEARCH

Open Access



Biochanin A modulates steroidogenesis and cellular metabolism in human granulosa cells through TAS2Rs activation: a spotlight on ovarian function

Francesca Paola Luongo^{1*}, Sofia Passaponti², Alesandro Haxhiu¹, Irene Ortega Baño¹, Rosetta Ponchia¹, Giuseppe Morgante¹, Paola Piomboni^{1*}  and Alice Luddi¹

Abstract

Background Endocrine-disrupting chemicals (EDCs) interfere with the endocrine system and negatively impact reproductive health. Biochanin A (BCA), an isoflavone with anti-inflammatory and estrogen-like properties, has been identified as one such EDC. This study investigates the effects of BCA on transcription, metabolism, and hormone regulation in primary human granulosa cells (GCs), with a specific focus on the activation of bitter taste receptors (TAS2Rs).

Methods Primary human GCs from 60 participants were treated with 10 μ M BCA, and selective antagonists were used to block TAS2R activation. The study assessed the expression of *TAS2R14* and *TAS2R43*, and analyzed the impact on *StAR* and *CYP17A1* gene expression. Intracellular calcium levels, lipid droplet size, and mitochondrial network complexity were measured to evaluate cellular metabolism and energy dynamics.

Results BCA treatment significantly upregulated *TAS2R14* and *TAS2R43* expression, leading to a 70% increase in *StAR* mRNA levels and a twofold increase in *CYP17A1* expression ($p < 0.05$). These effects were reversed by *TAS2R* antagonists. Additionally, BCA treatment decreased intracellular Ca^{2+} levels ($p < 0.01$) and reduced lipid droplet size ($p < 0.001$), both of which were counteracted by antagonists. Enhanced mitochondrial network complexity ($p < 0.001$) was also observed, suggesting increased mitochondrial fusion and improved cellular energy dynamics.

Conclusion The findings indicate that BCA modulates transcriptional and metabolic processes in GCs through the activation of TAS2Rs, highlighting their role in endocrine regulation. The statistically significant results emphasize the relevance of further exploring the effects of EDCs like BCA on reproductive health. Collaborative research efforts are essential to address and mitigate the adverse impacts of EDCs on fertility.

Keywords EDCs, Granulosa cells, TAS2Rs, Steroidogenesis, Biochanin A, Mitochondria

*Correspondence:

Francesca Paola Luongo
francesca.luongo@unisi.it
Paola Piomboni
piomboni@unisi.it

¹ Department of Molecular and Developmental Medicine, Siena University, Siena 53100, Italy

² Department of Life Sciences, University of Siena, Siena 53100, Italy

Introduction

Endocrine-disrupting chemicals (EDCs) are environmental contaminants known to interfere with the endocrine system, leading to various adverse effects on reproductive health and development. Recent declines in male and female fertility have been associated with exposure to various EDCs [1]. These compounds can mimic or



© The Author(s) 2025. **Open Access** This article is licensed under a Creative Commons Attribution-NonCommercial-NoDerivatives 4.0 International License, which permits any non-commercial use, sharing, distribution and reproduction in any medium or format, as long as you give appropriate credit to the original author(s) and the source, provide a link to the Creative Commons licence, and indicate if you modified the licensed material. You do not have permission under this licence to share adapted material derived from this article or parts of it. The images or other third party material in this article are included in the article's Creative Commons licence, unless indicated otherwise in a credit line to the material. If material is not included in the article's Creative Commons licence and your intended use is not permitted by statutory regulation or exceeds the permitted use, you will need to obtain permission directly from the copyright holder. To view a copy of this licence, visit <http://creativecommons.org/licenses/by-nc-nd/4.0/>.

block hormones, disrupt their production, or interfere with their signalling pathways, thereby impacting crucial physiological processes [2]. In females, EDCs have been implicated in numerous reproductive health issues, including a reduced number of viable oocytes, early onset of puberty, limited reproductive lifespan, complications in embryo implantation, endometriosis, and fibroids [3–5]. The growing body of evidence linking EDCs to reproductive disorders highlights the importance of understanding their mechanisms of action at the cellular and molecular levels [6, 7]. Phytoestrogens are the most common natural EDCs, plant-derived compounds found in food and drinks that mimic or interact with estrogenic hormones due to their structural similarity to 17β -estradiol, the primary female sex hormone [8]. Among these, the isoflavone Biochanin A (BCA), known for its anti-inflammatory and estrogen-like properties [9], is also a natural bitter compound that acts as a ligand for taste bitter receptors (TAS2Rs), a specific subset of GPCRs traditionally associated with bitter taste perception [10–12].

In previous studies, BCA demonstrated to link and activate TAS2R14 and TAS2R39, as other flavonoid compounds [10]. TAS2Rs are implicated in regulating various physiological functions, including hormone biosynthesis, cellular metabolism, and even immune responses [13, 14]. Upon activation, TAS2Rs can initiate multiple intracellular signaling cascades, including those involving calcium mobilization and cAMP production [15]. Notably, taste receptors are expressed not only in taste buds but also in non-gustatory tissues, including reproductive organs [13, 16, 17]. In the ovary, particularly in granulosa cells, TAS2Rs are crucial for follicle development and steroidogenesis [12, 18, 19]. Still, while their activation's exact effect on steroidogenesis remains unclear, some data suggest it may inhibit progesterone production, potentially through NO/cGMP and apoptotic signaling [20]. Considering this, the binding of EDCs to TAS2Rs could potentially lead to altered signaling and dysregulation of critical processes like steroidogenesis, highlighting the EDC's potential to influence reproductive health via TAS2R pathways. Despite the natural disruptor, BCA has been extensively studied concerning cancer and cardiovascular health [21], its possible influence on reproductive health, particularly through its interaction with novel TAS2R-induced signaling pathways, remains underexplored. We recently demonstrated that BCA is a potent agonist of TAS2Rs, as it effectively induces their expression in hGL5 cells—an immortalized cell line that closely mirrors the characteristics of primary follicular granulosa cells [12]. Therefore, to fully understand the physiological impact of BCA through these receptors on ovarian steroidogenesis, blockers of TAS2Rs are propelling to the

forefront of investigations in the latest studies. One of the most known TAS2R antagonists p-(dipropylsulfamoyl) benzoic acid (Probenecid). Probenecid inhibits TAS2R16, 38 and 43 through an allosteric reaction mechanism. Probenecid is an FDA-approved inhibitor of the Multidrug Resistance Protein1 (MRP1) transporter, that is clinically used to treat gout in humans or is co-administered with antibiotics and chemotherapeutics to reduce their excretion [22]. It selectively inhibits the binding of bitter ligand β -glucopyranosides including salicin, arbutin, and phenyl- β -d-glucopyranoside [23]. 4-sulfamoyl benzoic acid (SBA) is a probenecid analogue, reported as a TAS2R14 antagonist, so it competes with caffeine, which is one of its agonists [24]. Finally, (R)-citronellal is reported to act as a general allosteric inhibitor of TASR43 and TASR46, especially studied for its ability to fully block caffeine-induced calcium channels in the cells expressing those receptors [25]. Although BCA has been widely researched in the context of cancer and cardiovascular health, its possible impact on reproductive health, especially through its interaction with newly discovered TAS2R-induced signaling pathways, has not been thoroughly investigated. Therefore, this study aims to investigate the effect of the natural endocrine disruptor BCA on ovarian steroidogenesis in primary granulosa cells.

The findings of this study demonstrate that BCA activates TAS2Rs in GCs, leading to a notable upregulation of *StAR* and *CYP17A1* gene expression, increased estrogen secretion, and decreased progesterone levels. Additionally, BCA treatment results in reductions in intracellular Ca^{2+} levels and lipid droplets, while enhancing mitochondrial network complexity. Taken together, these results verified a crucial role for endocrine disruption in granulosa cells, revealing how bitter taste receptors specifically influence endocrine regulation. The findings offer valuable insights into the complex effects of endocrine disruptors, suggesting potential new broader implications of EDCs on reproductive health.

Materials and methods

Study design and human biological sample collection

The goal of this study was to evaluate the effect of BCA as an EDC on steroidogenesis and TAS2R regulation in human primary GCs. The cells were obtained from 60 women who had undergone in vitro fertilization at Siena University Hospital's Assisted Reproduction Unit. All participants gave written, informed consent for the use of their samples and data. The study complied with the Declaration of Helsinki and was approved by the University of Siena's ethical committee. (CEAVSE, Protocol number 18370, 2 October 2020). This study was performed following good clinical practice guidelines and written informed consent was obtained from

all patients. In all cases, the reason for having IVF was male infertility factor. The laboratory investigations were carried out blindly.

Human primary granulosa cells isolation and culture

After follicular fluid samples were collected, GCs were isolated from follicular fluid according to a previously described procedure [26]. The collected GCs were cultured for 1–2 days before the treatments at 37 °C and (5% CO₂), in Dulbecco Modified Eagle Medium (Invitrogen) containing 10% fetal bovine serum, 2 mmol/L L-glutamine, 100 U/mL penicillin, and 100 µg/mL streptomycin and treated/stored according to the analyses.

Cell proliferation assay and treatment protocols for biochanin a and antagonists

The most suitable GC concentration for experimental testing was determined using the Cell Counting Kit-8 (CCK-8, Abcam, Cambridge, UK) according to the manufacturer's instructions. Eight replicates were measured for each cell concentration, and the average data were used to create the calibration curve. The cytotoxicity of BCA and its antagonists —PRO, SBA, and CITRO— was assessed by measuring the viability of the treated GC using cell counting kit-8 after overnight incubation at 37 °C and (5% CO₂). All of them were purchased from Sigma Aldrich (Madrid, Spain). These compounds were dissolved in dimethyl sulfoxide (DMSO) and diluted in the media containing Dulbecco's Modified Eagle Medium (DMEM, 1X), containing fetal bovine serum (FBS) (10%), L-glutamine (1%), penicillin/streptomycin (1%), non-essential amino acids (1%) not exceeding a final DMSO concentration of 0.1% (v/v) to avoid the toxic effect of the cells. Different concentrations of each compound were tested, considering optimal TAS2R stimulation concentrations reported in the literature. The highest non-toxic doses of these compounds were selected based on the brief 24-h exposure period. The absorbance was measured after 4 h incubation (37 °C, 5% CO₂) with CCK-8 (10 µL). Four wells per compound were analyzed, and the average absorbance was calculated. Background absorbance from wells with media but no cells were subtracted from the readings of the test wells. Additionally, wells with cells but no stimulation served as a control group for assessing cytotoxicity. Based on the cytotoxicity results, the treatment conditions were established as follows: Untreated (DMSO only), BCA 10 µM, BCA 10 µM + PRO 1 mM, BCA 10 µM + SBA 30 µM, CITRO 150 µM, for 24 h.

Mitotracker staining and image processing using the mitochondria analyzer

GCs were plated on a coverslip, treated for 24 h treatments and incubated with MitoTracker[®] Red CMXRos probes at 37 °C for 15 min. This probe diffuses across the plasma membrane and accumulates in active mitochondria. After incubation, cells were fixed with Paraformaldehyde 4% for 15 min at RT, washed 3 times with PBS 1X and counterstained with DAPI. The coverslips were mounted and images were captured using a Leica 6500 microscope equipped with LAS software. Images were analyzed using Mitochondria Analyzer, an ImageJ plugin for processing and analyzing fluorescent mitochondria. This plugin requires image thresholding to quantify the morphological features of the identified mitochondrial structures, carefully setting a comprehensive set of parameters to mathematically describe key aspects of mitochondrial morphology. With the 2D approach, mitochondrial size is characterized by area and perimeter, while the shape is defined by form factor (FF) and aspect ratio (AR). We assess the overall connectivity and complexity of the mitochondrial network by analyzing the skeletonized network, measuring the number of branches, branch junctions, and the total length of the branches (Chaudhry, Shi, and Luciani, 2020).

RNA extraction, complementary DNA preparation and qPCR

Total RNA was isolated from GCs with a RNeasy Micro kit (Qiagen, Hilden, Germany), according to the manufacturer's instructions. At the end of the protocol, RNA extracted from each sample was diluted in a final volume of 20 µL of water. The purity and the concentration of RNA were evaluated by reading on NanoDrop[®] ND-100 UV-vis Spectrophotometer (Thermo Fisher Scientific, Waltham, MA, USA). 200 ng of the extracted RNA was reverse transcribed into cDNA, using the iScript gDNA Clear TM cDNA Synthesis Kit (Bio-Rad Laboratories, Hercules, CA, USA). We started with a treatment of samples with a master mix of DNase to remove contaminating genomic DNA. To inactivate the effect of DNase, the samples were incubated in a thermal cycler at 25 °C for 5 min and at 75 °C for another 5 min. 4 µL of the iScript reverse Transcription Supermix was added to each sample; they were then incubated in a thermal cycler (5 min at 25 °C, 20 min at 46 °C, 1 min at 95 °C).

Gene expression of *TAS2R14*, *TAS2R43*, *StAR*, *CYP17A1* and *GADPH* was measured by Real-Time qPCR. The PCR mix consisted of Green Master Mix FAST ROX 2X (Genaxxon Bioscience GmbH, Ulm, Germany), primers 1X, cDNA and water. The PCR conditions were 3 min at 95°C, followed by 40 cycles of

denaturation at 95°C for 10 s, annealing at 60°C or 58°C for 10 s and primer extension at 72°C for 20 s. To normalize the expression levels of the gene transcripts of GCs a simultaneous mRNA expression profiling of the housekeeping gene *GADPH* was also performed in all the analyzed samples. All amplification reactions were conducted in triplicate by qRT-PCR on a CFX Connect Real-Time PCR Detection System (Bio-Rad Laboratories) gene-specific primer sets used in this study are listed in Supplementary Table 1. Melting curve analysis was also performed to confirm the specificity of the products obtained. Changes in gene expression levels were calculated by the $2^{-\Delta\Delta C_t}$ method.

Western blot analysis

Western blotting was performed as previously described [27]. Briefly, 50 µg of total proteins were denatured, separated on 10% polyacrylamide gel and then transferred onto a nitrocellulose membrane (GE Healthcare, Chicago, IL, USA). After blocking for 1 h in 5% nonfat dry milk, the membrane was incubated overnight at 4 °C with primary antibodies (see Supplementary Table 2) diluted in 1% nonfat dry milk/TTBS (TBS containing 0.2% Tween 20). After washing in TTBS, the membrane was incubated with the appropriate horseradish peroxidase (HRP)-conjugated secondary antibody (see Supplementary Table 2). Membranes were stripped using a harsh stripping buffer containing 62.5 mM Tris-HCl (pH 6.8), 2% SDS, and 100 mM β-mercaptoethanol. Membranes were incubated in the buffer at 37 °C for 15–20 min with gentle agitation, followed by three washes in TBS-T (5 min each). Stripped blot did not have any remaining background staining and therefore could provide a true assessment of other antibodies. After stripping, membranes were blocked in 5% BSA or non-fat milk for 1 h and reprobed using standard WB procedures. Immunostained bands were visualized by chemiluminescence with ImageQuant LAS 4000 (GE Healthcare).

Immunofluorescence analysis

Immunofluorescence was performed as previously described [28]. Antibodies used in this study are listed in Supplementary Table 2.

Oil red O (ORO) staining

The amount of lipids accumulated in GCs was evaluated using the Oil red O staining method according to a previously described protocol [29], with slight modifications. 0.5 g of ORO were resuspended in 100 mL of isopropanol (ORO stock solution). The working solution was prepared with 30 mL of this stock diluted with 20 mL ddH₂O (ORO-saturated solution). Following EDC

treatments, cells were washed 3 times with PBS and fixed with 4% paraformaldehyde for 10 min. Cells were then washed twice with PBS and were subsequently stained with Oil red O (Sigma Aldrich) in the dark for 15 min at room temperature. Thereafter, cells were stained with hematoxylin, washed with PBS, and photographed using a phase contrast microscope (Olympus, Tokyo, Japan). For the quantification of the droplets, cells were plated in 96 wells, with treatments conducted in replicates of 8. The protocol was followed as outlined, with a modification in the final step, where isopropanol was added to extract Oil red O. Supernatant was subjected to determination of optical density (OD) value at 540 nm using the automatic enzyme immunoassay analyzer.

Progesterone and estradiol quantification

To assess the production of P4 and (Estradiol) E2, 72-hour preincubation period of granulosa cell monolayers was conducted, with medium replacement occurring after 48-h and again after 24-h (1 mL medium per well) in the culture medium for 24-h with BCA antagonist and the control. The P4 and E2 assays demonstrated sensitivities of 6 and 1 pg/tube, respectively. Serial dilutions of medium samples exhibited a similar pattern to the standard curves for the steroids under investigation. All analyses were conducted in triplicate. The concentration of steroid hormones in the spent culture medium was measured by Immulite 2000 (Siemens).

Intracellular cAMP assessment

Free cAMP production (nM) in the samples was assessed using an ELISA cAMP Direct Immunoassay Detection Kit (Abcam, ab138880) according to the manufacturer's instructions. ELISA plates were analyzed using a Synergy MX plate reader (BioTek, USA). Only ELISA plates that had R²>0.90 in their standard curve were included in the analysis. ELISA assay was performed in duplicate for each sample analyzed.

ROS detection

Carboxy-2',7'-dichlorodihydrofluorescein diacetate dye (DCFH-DA) (Life Technologies Corp., Carlsbad, CA) was used to detect intracellular H₂O₂. This dye is oxidized by H₂O₂ to the highly fluorescent derivative 2',7'-dichlorofluorescein (DCF). Detection of intracellular ROS in GCs by DCFH-DA assay was assessed. Briefly, after removing the medium, cells were incubated with DCFH-DA solution (10 µM in PBS) at 37 °C for 15 min. Then they were centrifuged to remove the DCFH-DA solution and resuspended with PBS. Fluorescence was measured using excitation and emission wavelengths of 480 and 520 nm, respectively (Synergy HTX multi-mode reader, BioTek,

Winooski, VT, USA), and normalized to the number of live cells. All experiments were repeated three times.

Intracellular calcium measurement

Intracellular Calcium levels were assessed using a Colorimetric Calcium Assay Kit (Assay Genie MAES0091). The cells were collected and washed with PBS (0.01 M, pH 7.4) 1–2 times. The sample was then centrifuged at 1000 g for 10 min. The supernatant was discarded, and the cell sediment was retained. Homogenization medium was added at a ratio of cell number (1×10^6) to deionized water (μL) = 1:200. The sample was sonicated in an ice water bath. After this, centrifugation was carried out at 10,000 g for 10 min. The supernatant was taken and preserved on ice for detection. If detection was not performed on the same day, the cell sample (without homogenization) could be stored at -80°C for up to one month.

Calcium content (mmol/g prot) was calculated using the following formula: $(\Delta A_{610} - b) \div a \times f \div \text{Cpr}$.

Where: a: The slope of standard curve; b: The intercept of standard curve; f: Dilution factor of sample before test; Cpr: Concentration of protein in sample, gprot/L ΔA_{610} : Absolute OD (ODSample – ODBlank). Intracellular Calcium levels were measured in duplicate for each sample analyzed.

Statistical analysis

Statistical analyses were performed with GraphPad Prism 9.0 (GraphPad Software, San Diego, CA, USA). All data obtained from the experiments were analyzed for normality using the Shapiro-Wilk, followed by the parametric or non-parametric tests, ANOVA or Kruskal-Wallis respectively, as appropriate. Densitometric analyses were completed using ImageJ software. Statistical significance was set at $p < 0.05$.

Results

BCA affects TAS2R14 and TAS2R43 expression and regulates steroidogenesis

To clarify the association between the natural endocrine disruptor BCA and *TAS2Rs* expression in human GCs, we first tested the cytotoxic effect of this compound on human primary GCs isolated from the follicular fluid of women undergoing IVF. BCA did not affect the viability of GCs. After determining the optimal concentration, we observed that adding BCA to human primary GCs led to the induction of both *TAS2R14* and *TAS2R43* expression (Fig. 1A–B). This effect was blocked by sulfamoyl-benzoic acid (SBA), a selective antagonist of *TAS2R14* [24], and by both probenecid

(PRO) and citronelle (CITRO), two selective antagonists of *TAS2R43* [25, 30] (Fig. 1A–B). Notably, when administered individually, PRO, SBA, and CITRO did not influence *TAS2R* expression, confirming that the observed effects are attributable to receptor blockade rather than any direct action of the antagonists themselves (Supplementary Fig. 1).

Our data also provide evidence that PRO and CITRO can efficiently inhibit *TAS2R14*, and that SBA can counteract the effect of BCA in inducing *TAS2R43* expression. All antagonists (PRO, SBA and CITRO) significantly decreased *TAS2Rs* expression, thus confirming this EDC directly affects the *TAS2Rs* pathway.

Previous research has shown that *TAS2R* agonist saccharin can modulate factors involved in steroidogenesis [20]. We, therefore, assessed the expression of the steroidogenic acute regulatory protein (*StAR*), which transports cholesterol to the inner mitochondrial membrane and is a rate-limiting regulator of steroid production (Christenson and Strauss, 2000). When stimulated with BCA, GCs had a 70% increase in *StAR* mRNA levels compared to unstimulated GCs ($p < 0.05$). We further found that 17α -hydroxylase (*CYP17A1*), a critical enzyme in the steroidogenesis pathway, showed a two-fold increase in expression when treated with BCA, as compared to the control. However, when combined with antagonists, the expression of both *StAR* and *CYP17A1* was significantly reduced ($p < 0.05$).

After 24-h exposure to BCA and *TAS2R* antagonists, we also measured GC's steroid hormones estrogen and progesterone levels (Fig. 1E–F). BCA treatment resulted in a significant decrease in progesterone secretion ($p < 0.0001$), an effect that was notably counteracted by both SBA and CITRO ($p < 0.001$), while PRO did not show any statistically significant effect (Fig. 1E). In contrast, BCA treatment led to a substantial increase in estrogen secretion ($p < 0.0001$), which was partially reduced by the antagonist SBA and CITRO (Fig. 1F).

Several studies have demonstrated that ERK1/2 is involved in regulating progesterone production in granulosa cells [31, 32]. To further confirm BCA's role in modulating steroidogenesis in these cells, we assessed ERK1/2 activation by immunoblotting (Fig. 2A–B–C–D) using a phospho-specific antibody that detects dually phosphorylated ERK1 and ERK2, a widely accepted method for indirectly measuring ERK activity. As shown in Fig. 2C, the levels of activated ERK (pERK) significantly decreased following BCA treatment ($p < 0.05$). Additionally, intracellular cAMP levels were measured in the same cells, revealing a decrease in this second messenger in BCA-treated cells (Fig. 2E), partially reversed by *TAS2R* antagonists. This finding aligns with the known ability

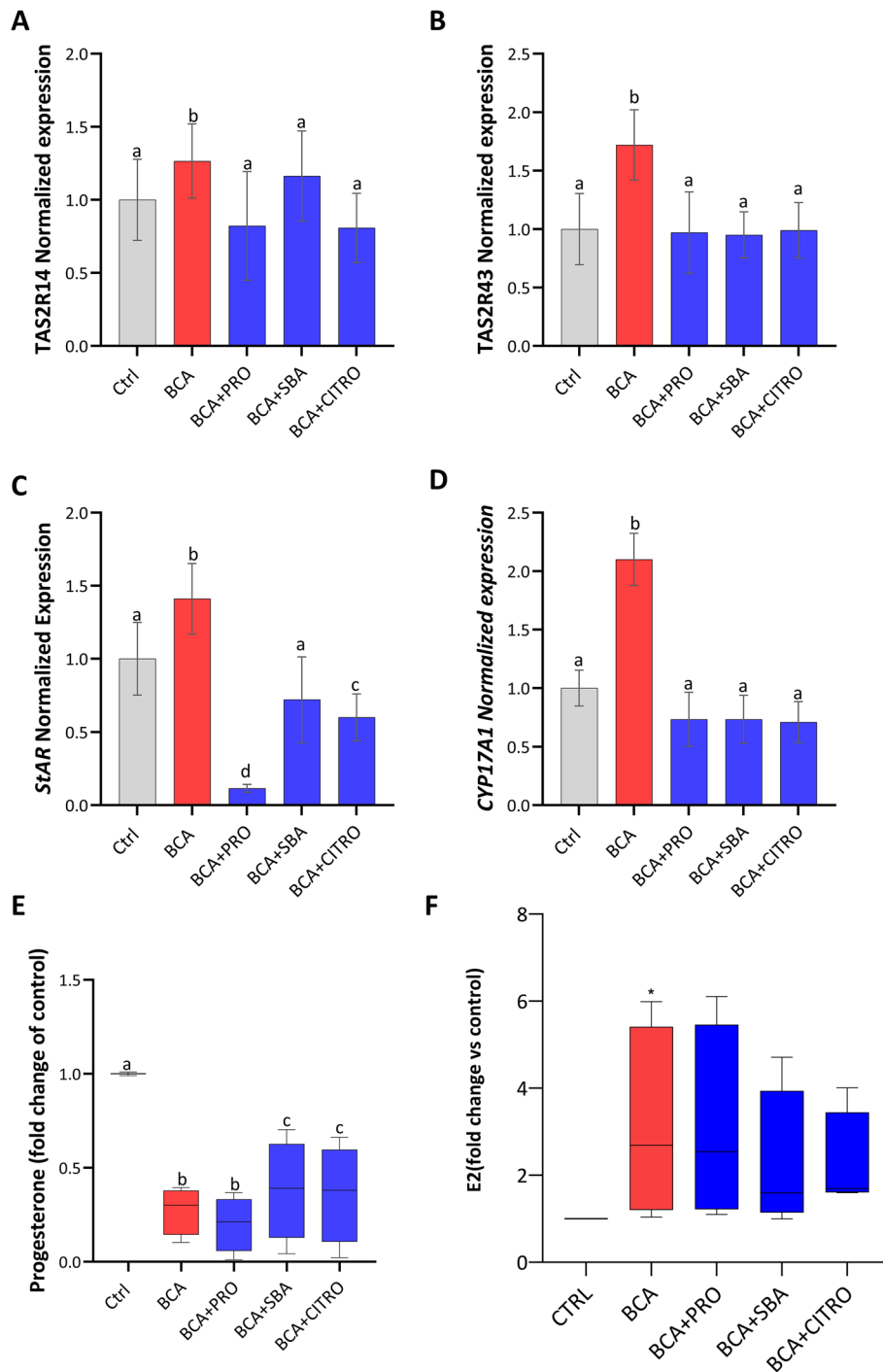


Fig. 1 Relative mRNA expression levels of *TAS2R14* (A), *TAS2R43* (B), *StAR* (C), and *CYP17A1* (D) in GCs ($n=30$) were measured under various conditions: untreated (Ctrl), treated with BCA 10 μ M for 24-h, and co-treated with BCA 10 μ M plus either PRO 1 mM (BCA + PRO), SBA 30 μ M (BCA + SBA), or CITRO 150 μ M (BCA + CITRO) for 24-h. Antagonists were preincubated for 1 h before the addition of BCA. The means \pm SD mRNA levels are expressed as a relative fold change compared to Ctrl after normalizing on the housekeeping gene GADPH. Statistical significance was calculated by Ordinary One-way ANOVA test (multiple comparisons) and indicated with letters. **E-F** Progesterone (E) and E2 (F) secretion from GCs, expressed as fold change relative to the control (set to 1). Different letters and * indicate statistically significant differences ($p \leq 0.05$)

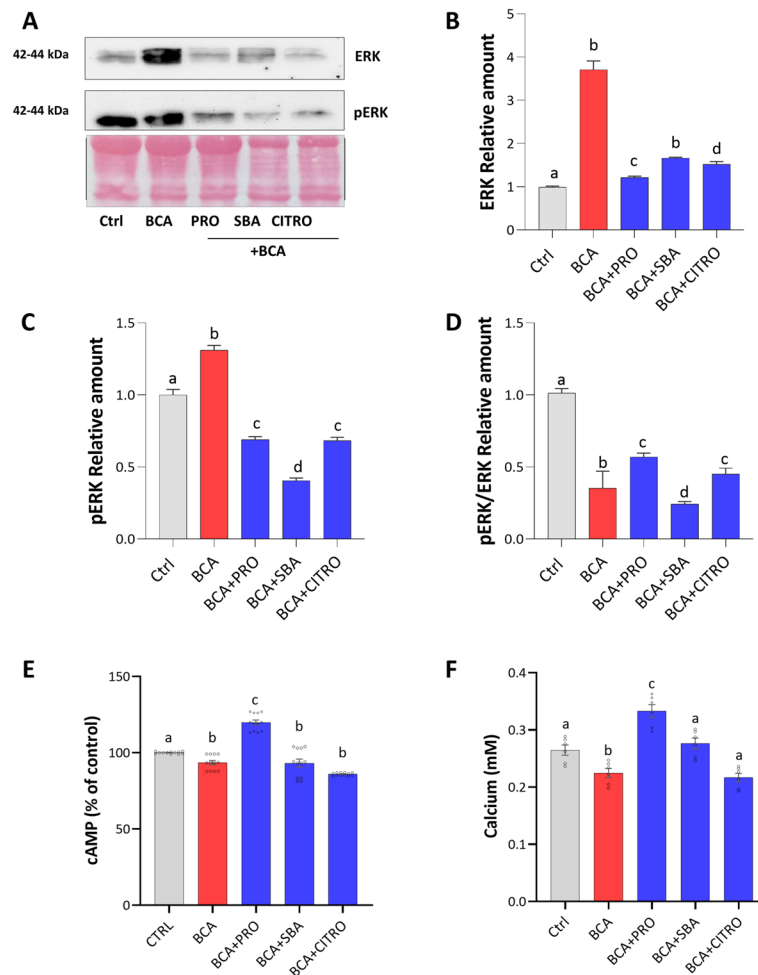


Fig. 2 **A** Representative image of western blot analysis of pERK 1/2 and total ERK 1/2 expression in GCs ($n=20$) were measured under various conditions: untreated (Ctrl), treated with BCA 10 μ M for 24-h, and co-treated with BCA 10 μ M plus either PRO 1 mM (BCA + PRO), SBA 30 μ M (BCA + SBA), or CITRO 150 μ M (BCA + CITRO) for 24-h. Antagonists were preincubated for 1 h before the addition of BCA. Equal protein loading of the preparations was verified using Ponceau staining. The image is representative of three independent experiments. **B-D** Computer-assisted semi-quantitative analysis of the overall relative intensity of the bands. The intensity was measured (pixel/mm²) and then normalized relative to Ponceau staining. Values are expressed as fold change as respect to the control. Different letters indicate statistically significant differences ($p \leq 0.05$). **E** Intracellular cAMP concentration in GCs. Results (expressed as mean \pm SD) are expressed as a percentage relative to untreated cells, which are set at 100%. Experiments were each performed in duplicate. **F** Intracellular Calcium levels (mM) in GCs according to different treatments, measured in duplicate. Statistical analyses were conducted using GraphPad Prism 9, employing a one-way analysis of variance (ANOVA) followed by Tukey's post hoc test to assess significant differences. Different letters indicate statistically significant differences ($p \leq 0.05$)

of TAS2Rs to activate PDE [33] and confirms that BCA, via TAS2R receptors, can modulate steroidogenesis in human granulosa cells. The same trend was obtained when the levels of intracellular calcium were measured (Fig. 2F).

BCA affects lipid droplet (LD) homeostasis

OilRed O staining, which selectively targets neutral lipids, revealed an increase in the cytoplasmic accumulation of intracellular lipids in the GCs treated with BCA

compared to untreated cells (Fig. 3A). However, this difference doesn't reach statistical significance ($p > 0.05$). Administration of PRO and SBA, resulted in a reduction in lipid content, as shown in Fig. 3B. In contrast, CITRO, didn't counteract the lipid-accumulation effect of BCA. Interestingly, further analysis of lipid droplet morphology in BCA-treated GCs showed smaller, predominantly spherical lipid droplets ($p < 0.001$) (Fig. 3C). The treatment with TAS2Rs antagonists significantly increased the size of lipid droplets. ($p < 0.001$).

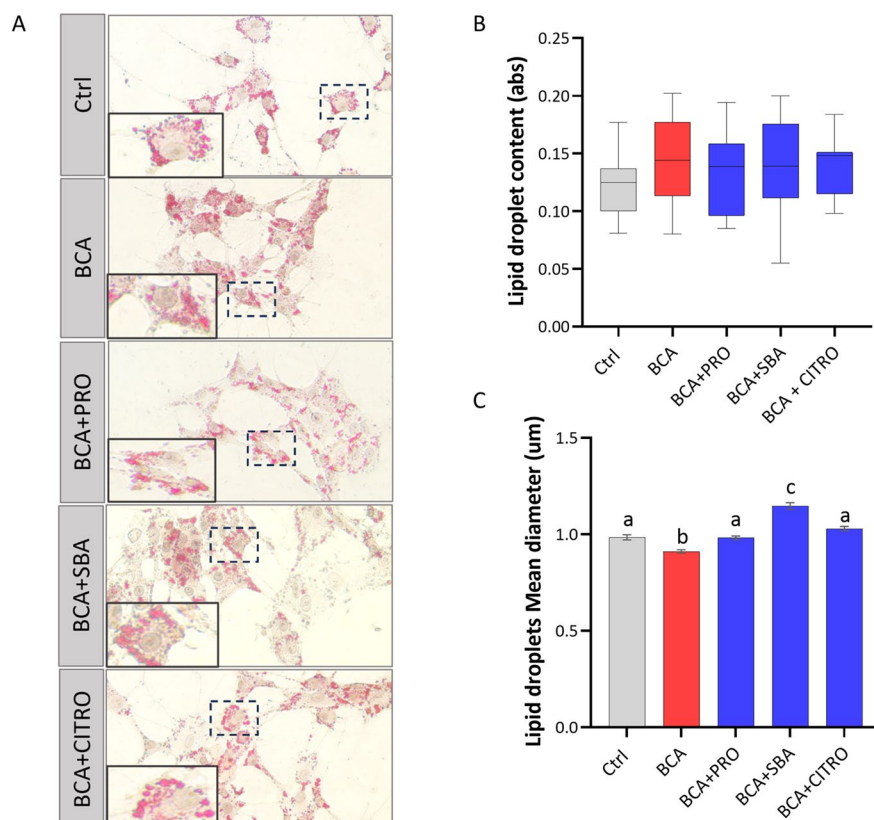


Fig. 3 Lipid analysis through Oilred O staining ($n=10$). **A** Representative images of Oilred O staining in Ctrl, BCA and antagonists PRO, SBA and CITRO 1-h pretreatment before BCA addition. **B** Lipid content relative to the Ctrl **(C)** GC lipid droplets mean diameter measure in μm . Results are presented as means \pm standard deviations of at least three experiments. Statistics were performed in GraphPad Prism 9 using one-way analysis of variance (ANOVA) with Tukey's post hoc test to assess significant differences. Different letters indicate statistically significant differences ($p \leq 0.05$)

TAS2R antagonist reverts the effect of BCA on mitochondrial dynamic

Mitochondria are crucial organelles where steroidogenesis begins, making their proper organization essential for accurate hormone production. Evaluating the mitochondrial network is key to understanding mitochondrial dynamics. The Mitochondrial Analyzer software excels in detecting morphological differences and structural features, providing an accurate assessment of mitochondrial organization.

Using this approach, we observed that the number of mitochondria per cell remained unchanged, while BCA treatment significantly increased the mean mitochondrial area ($p < 0.001$) compared to the control, indicating activation of mitochondrial fusion (Fig. 4A-B). This effect was effectively reversed by TAS2Rs antagonists ($p < 0.001$), which, counteracted the BCA-induced changes and appeared to inhibit mitochondrial fusion (Fig. 4A-B).

In addition to changes in mitochondrial number, area, and length, it is essential to investigate alterations in mitochondrial networks, as energy metabolism

is closely linked to these network modifications [34]. BCA treatment significantly increased both the number of branches and the total branch length per mitochondrion, indicating enhanced network complexity (Fig. 4C-D; $p < 0.001$). Conversely, antagonist treatment led to a significant reduction in both branch number (Figure A; $p < 0.02$) and total branch length (Fig. 4C-D; $p < 0.009$). Finally, we measured the average form factor to quantify overall mitochondrial network complexity, where higher values denote more intricate networks and lower values indicate simpler ones. As shown in Fig. 4F, the average form factor is significantly higher in BCA-treated GCs, further confirming the increase in network complexity (Fig. 4E; $p < 0.001$). The antagonists effectively counteracted BCA-induced changes, resulting in a notable decrease in mitochondrial network complexity as well as a higher level of potential energy.

The presence of a robust mitochondrial network resulting from the mitochondrial fusion process contributes to improved energy efficiency as well as to a more efficient oxidative phosphorylation (OXPHOS) [35]. By contrast, fission is related to increased

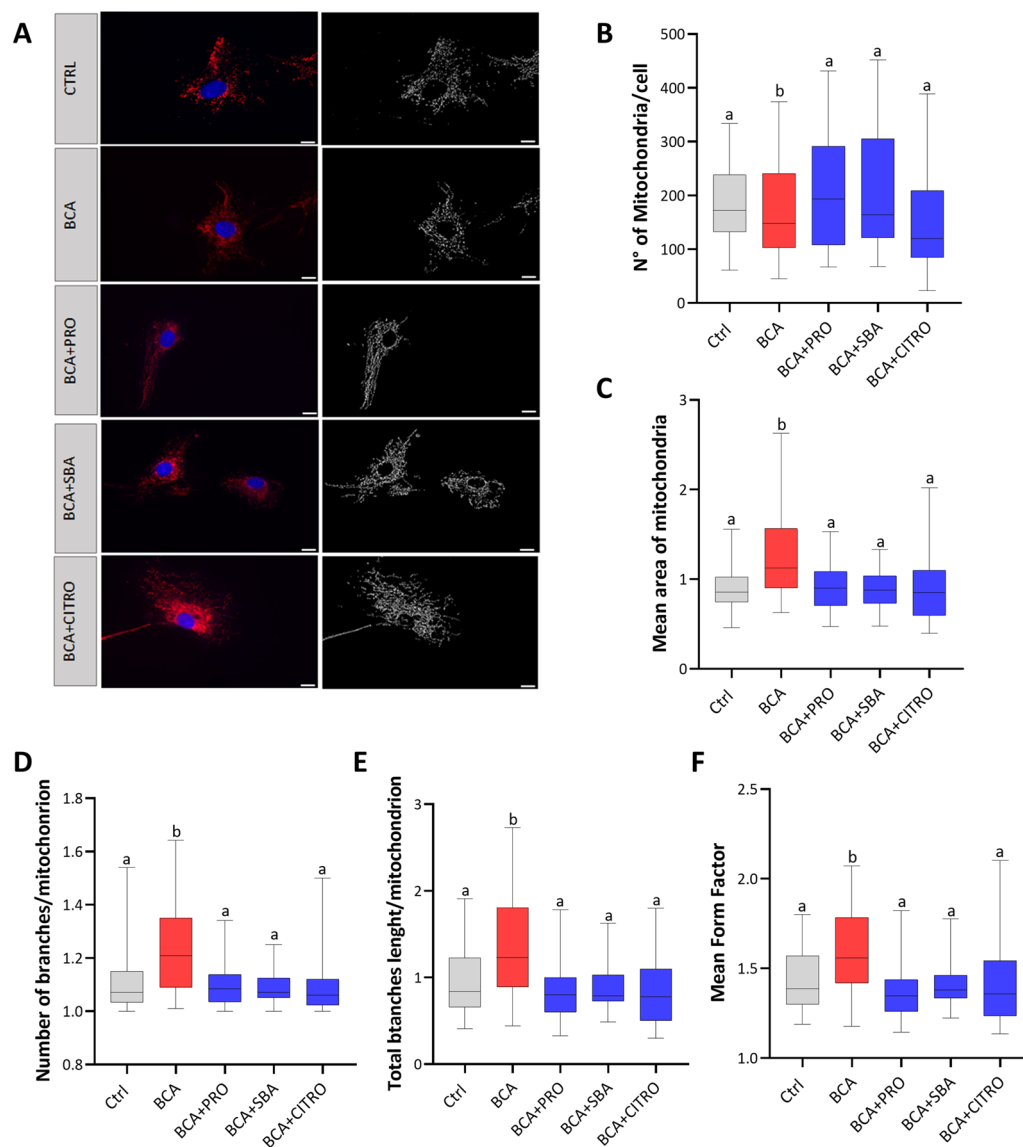


Fig. 4 **A** Mitochondrial staining (red) of GCs ($n = 10$) exposed to different compounds. Nuclei were DAPI-stained (blue). On the right part example of the skeletonization of the image required by the Software. Ctrl = untreated cell (control). Magnification: 630 \times . Staining pictures are representative of five independent experiments. Results from mitochondrial network analysis in GCs using Mitochondria Analyzer. A summary statistic box plots show the median (horizontal lines), first to third quartile (box), and the most extreme values within 1.5 times the interquartile range (vertical lines) for: the Number of mitochondria per cell (**B**), Mean area of mitochondria (**C**), N $^{\circ}$ branches per mitochondrion (**D**), total branches length per mitochondrion (**E**), mean form factor for all conditions (**F**). Different letters indicate statistically significant differences ($p \leq 0.05$)

uncoupling, and increased ROS production [36]. To validate the induction of mitochondrial fusion by the TAS2R agonist BCA, we assessed the level of ROS in treated GCs. The figure illustrates that the addition of BCA leads to a reduction in ROS production, partially counteracted by TAS2R selective antagonists, although statistical significance is not reached (Fig. 5A).

Immunoblot analysis of GC demonstrated high levels of COX4 expression, with BCA treatment resulting in a

significant increase in its relative abundance (Fig. 5B); this increase was not reversed by antagonist treatment. Immunofluorescent staining revealed that COX4 exhibited tight perinuclear clustering in untreated cells, while BCA treatment led to an expansion of mitochondria throughout the cytoplasm (Fig. 5C).

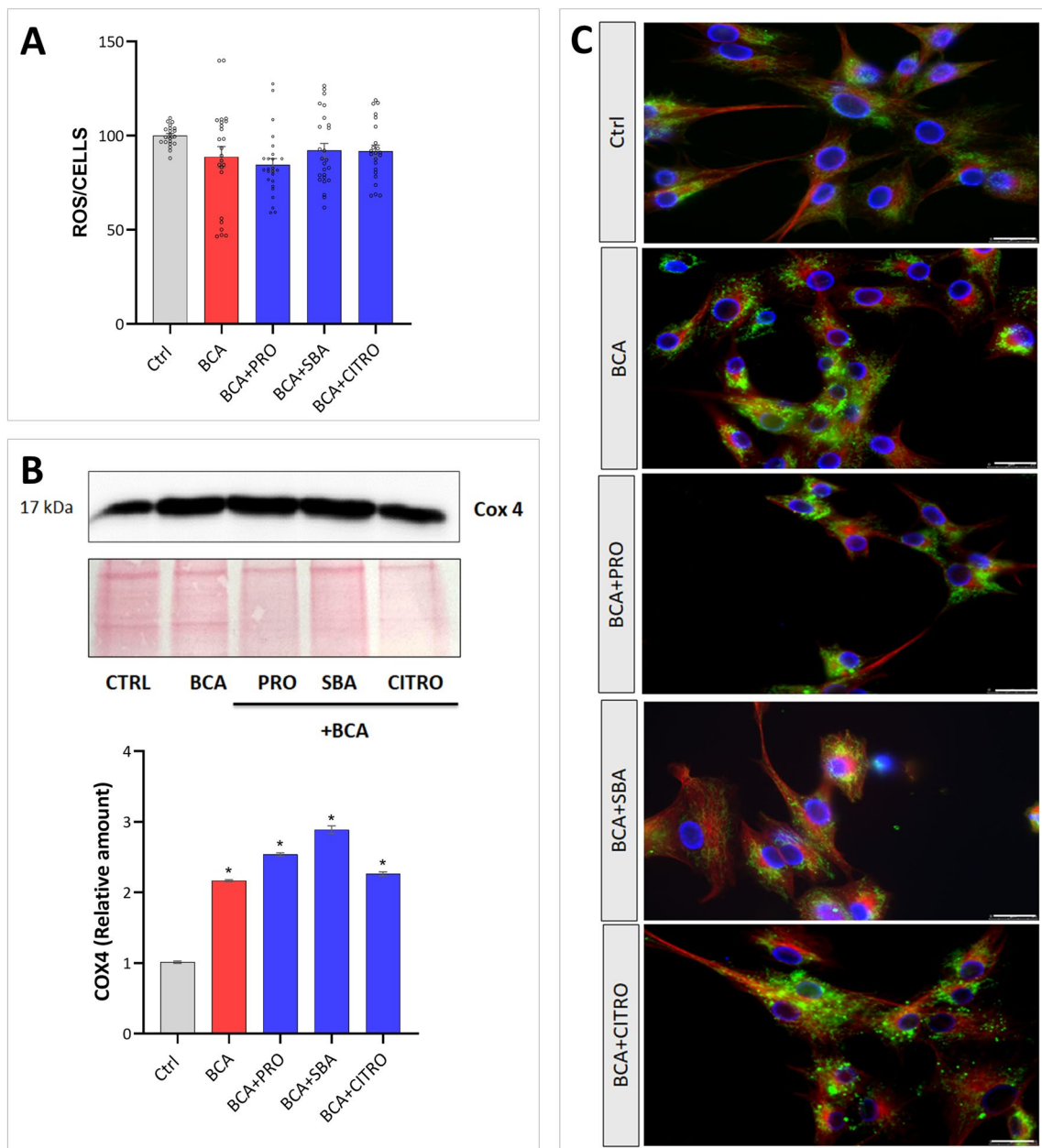


Fig. 5 **A** ROS/cell % over control ($n = 12$). The experiments were repeated for three times. **B** Representative image of western blot assay for COX4 in GCs untreated (CTRL), treated with 10 μM BCA or with BCA and TAS2R antagonist SBA, CITRO e PRO ($n = 5$). Band intensity, normalized to Ponceau staining, is reported as fold change relative to the control group. **C** Immunofluorescence detection of COX4 visualized in green and β-Tubulin (red) in GCs untreated (Ctrl), treated with 10 μM BCA or with BCA and TAS2R antagonist SBA, CITRO e PRO ($n = 10$). DAPI nuclear staining in blue. Scale bars represent 25 μm

Discussion

This study elucidates the impact of the natural endocrine disruptor BCA on granulosa cell function, emphasizing the critical mediating role of TAS2R receptors. Using specific TAS2R antagonists, we demonstrate that 10 μM BCA effectively activates TAS2Rs in primary GCs, resulting in a significant upregulation of the steroidogenic

enzymes *StAR* and *CYP17A1*. These enzymes, crucial in the early stages of steroidogenesis, act as specific and sensitive indicators of both estrogen and progesterone synthesis. Notably, they reflect the rate of progesterone synthesis, which occurs independently of other key steroidogenic enzymes like *CYP19A1*. Meanwhile, *CYP17A1* plays an indirect but critical role in estrogen production

by providing the androgenic substrates required for aromatization [37]. This approach enabled us to capture both the upstream and downstream effects of steroidogenesis in granulosa cells, providing a comprehensive view of the hormonal dynamics following BCA treatment. Specifically, we observed that BCA-induced upregulation of *STAR* and *CYP17A1* is associated with increased estrogen secretion and decreased progesterone levels. Direct hormone measurement provided a clear assessment of BCA's effects on granulosa cell steroidogenesis, eliminating potential biases related to post-transcriptional and translational regulation of enzyme expression.

In bovine granulosa cells, Biochanin A exhibits a dose-dependent, biphasic effect on steroidogenesis, stimulating progesterone production by 50% at 185 nmol/L, while inhibiting it at concentrations exceeding 176 nmol/L [38]. Our findings, showing a similar effect on steroidogenesis with BCA at a concentration of 10 μ M, reinforce these observations. Importantly, the effects of BCA are reversed by selective TAS2R inhibitors, confirming that BCA exerts its influence through bitter taste receptors.

While the precise impact of ovarian TAS2R activation on steroidogenesis is still unclear, evidence suggests that these receptors play a role in regulating hormone synthesis and balance by influencing steroidogenic pathways across various cell types [2, 7]. For instance, studies have shown that activating bitter taste receptors may inhibit progesterone production, possibly through NO/cGMP and apoptotic signalling pathways [20]. In the murine PCOS model, oral administration of KDT501, a ligand for the *TAS2R4* orthologue, effectively alleviated PCOS-related endocrine and metabolic disorders and restored reproductive function, surpassing the effects of the PPAR γ agonist; specifically, KDT501 reduced levels of testosterone and androstenedione without significantly affecting LH or FSH, and it also decreased hepatic lipid accumulation and body fat [18].

To elucidate the mechanisms underlying the BCA's effects, we demonstrate that BCA treatment significantly reduces levels of activated ERK (pERK). This finding is consistent with previous research showing that ERK1/2 plays a crucial role in regulating progesterone production in granulosa cells [39]. Notably, both ERK and PKA are critical mediators of optimal steroidogenesis, with ERK playing a pivotal role in correctly positioning StAR on the mitochondrial membrane [40, 41].

The observed decrease in ERK levels may explain the reduction in progesterone production, even with an increase in *StAR* transcription. In addition, our study identified a significant reduction in intracellular cAMP levels, a crucial second messenger in LH-induced steroidogenesis. These findings collectively highlight BCA's role in targeting key signaling pathways essential for

optimal steroidogenesis, likely through its interaction with TAS2R receptors.

The reduction in lipid droplet size following BCA treatment aligns with its known ability to inhibit lipid accumulation [42]. This finding also reinforces the role of TAS2Rs in modulating cellular metabolism and energy dynamics, in particular, suggesting that BCA might alter lipid storage or utilization, potentially impacting cellular energy balance and steroidogenesis [12, 43]. In this regard, TAS2R138 has been shown to promote the degradation of lipid droplets in neutrophils [44], further supporting its involvement in lipid metabolism.

We also provide clear evidence that BCA influences mitochondrial activity. Biochanin A has been shown to promote mitochondrial biogenesis and the production of functional mitochondria [45]. In our experimental model, BCA significantly increases COX4 levels, a key mitochondrial function marker [46]. The production of ROS is inversely correlated with COX4 levels, a key indicator of mitochondrial function; COX4 regulates BMI1 expression by reducing mitochondrial ROS production [47, 48].

Moreover, by using Mitochondrial Analyzer, we observed that BCA-treated cells exhibited increased mitochondrial network complexity, indicative of enhanced mitochondrial fusion—an essential process for steroid production [40].

It has been reported that cells exhibit higher respiratory activity and greater oxidative capacity when mitochondria are hyperfused [49], while fragmented mitochondria are linked to lower energy demand, reduced respiratory activity and increased cellular stress [49, 50].

A well-developed mitochondrial network, like the one induced by BCA treatment, is associated not only with mitochondrial fusion and increased OXPHOS capacity but also with changes in mitochondrial dynamics—such as density, number, and spatial distribution—that can influence mitochondria-driven ROS propagation [36, 51]. Our results showed that BCA treatment reduces ROS production, an effect that is partially offset by TAS2R selective antagonists, though this difference did not reach statistical significance.

Despite its promising *in vitro* effects, the relevance of Biochanin A (BCA) to *in vivo* ovarian function requires careful consideration. Given its low oral absorption and bioavailability, achieving a physiologically relevant concentration such as 10 μ M in human serum is unlikely under normal dietary conditions [52, 53]. In fact, the maximum plasma concentration of BCA achievable with a daily oral intake of 5–50 mg/kg body weight in rats is ≤ 1 μ M, which aligns with the typical physiologically relevant concentration [54]. Yet, this chronic, low-dose exposure can still yield significant biological effects over time, as seen in other isoflavones like

genistein and resveratrol. Indeed, chronic genistein intake in animal models has been shown to modulate hormone levels, reduce oxidative stress, and improve metabolic profiles, despite serum concentrations being in the nanomolar range [55]. Similarly, another phytoestrogen, resveratrol, demonstrates strong anti-inflammatory and antioxidant effects in vivo despite its low bioavailability, owing to its active metabolites and prolonged low-dose exposure [56]. BCA metabolites, including glucuronides and sulfates, are present in the serum and may contribute to its biological effects. While unmetabolized BCA is typically found at low serum concentrations (in the nanomolar range), these metabolites may enhance and prolong its activity. This is facilitated by enterohepatic circulation, a process that recycles metabolites back into the bloodstream, thereby extending their bioactive presence [52]. Thus, while the in vitro responses are promising, further research is needed to understand how BCA could impact ovarian function in a living organism.

Conclusion

In summary, this study offers a comprehensive analysis of how the natural endocrine disruptor BCA impacts primary GCs through TAS2R activation. The observed changes in hormone levels, cellular metabolism, and mitochondrial dynamics reveal the complex interplay between TAS2Rs and endocrine regulation. These findings underscore the importance of further research into the broader implications of EDCs on reproductive health, particularly highlighting how TAS2R can serve as a sentinel in reprotoxic studies. Understanding how TAS2R-mediated pathways might be targeted or modulated could be key to mitigating the adverse effects of these disruptors on fertility.

Supplementary Information

The online version contains supplementary material available at <https://doi.org/10.1186/s12958-025-01344-9>.

Supplementary Material 1.

Supplementary Material 2.

Acknowledgements

The authors would like to thank all individuals who participated in this study. We thank the University of Siena Open Access funding for partially supporting the APC fees.

Authors' contributions

F.P.L., A.L. and P.P. were involved in the study conception and design. G.M. and R.P. performed the clinical work and contributed to the acquisition of clinical samples and data. S.P., F.P.L. analysed the data and drafted the article. F.P.L., S.P., I.O.B., A.H., performed experiments on human samples. F.P.L., S.P., A.L. and P.P. were involved in manuscript editing and reviewing, and final approval of the

version to be submitted. All authors have read the final submission and agree to be accountable for their aspects of the work.

Funding

This work was supported by grants from University of Siena (PSR2023).

Data availability

No datasets were generated or analysed during the current study.

Declarations

Ethics approval and consent to participate

Written informed consent was obtained from all participants prior procedure and was approved by the University of Siena's ethical committee. (CEAVSE, Protocol number 18370, 2 October 2020).

Consent for publication

Written informed consent for publication was obtained from all participants.

Competing interests

The authors declare no competing interests.

Received: 29 October 2024 Accepted: 11 January 2025

Published online: 25 January 2025

References

- Amir S, Shah STA, Mamoulakis C, Docea AO, Kalantzi O-I, Zachariou A, et al. Endocrine disruptors acting on Estrogen and Androgen Pathways Cause Reproductive Disorders through multiple mechanisms: a review. *Int J Environ Res Public Health*. 2021;18:1464.
- Gore AC, Chappell VA, Fenton SE, Flaws JA, Nadal A, Prins GS, et al. EDC-2: the Endocrine Society's Second Scientific Statement on endocrine-disrupting chemicals. *Endocr Rev*. 2015;36:E1–150.
- Caserta D, Costanzi F, De Marco MP, Di Benedetto L, Matteucci E, Assorgi C, et al. Effects of endocrine-disrupting chemicals on endometrial receptivity and embryo implantation: a systematic review of 34 mouse Model studies. *Int J Environ Res Public Health*. 2021;18:6840.
- Panagopoulos P, Mavrogianni D, Christodoulaki C, Drakaki E, Chrelias G, Panagiotopoulos D, et al. Effects of endocrine disrupting compounds on female fertility. *Best Pract Res Clin Obstet Gynecol*. 2023;88:102347.
- Wenger JM, Marci R. Endocrine Disruption in Women: A Cause of PCOS, Early Puberty, or Endometriosis. In: Marci R, editor. *Environment Impact on Reproductive Health: A Translational Approach*. Cham: Springer International Publishing; 2023 [cited 2024 Aug 5]. pp. 89–111. Available from: https://doi.org/10.1007/978-3-031-36494-5_5.
- Caserta D, Mantovani A, Marci R, Fazi A, Ciardo F, La Rocca C, et al. Environment and women's reproductive health. *Hum Reprod Update*. 2011;17:418–33.
- Rattan S, Flaws JA. The epigenetic impacts of endocrine disruptors on female reproduction across generations†. *Biol Reprod*. 2019;101:635–44.
- Messina M, Mejia SB, Cassidy A, Duncan A, Kurzer M, Nagato C, et al. Neither soyfoods nor isoflavones warrant classification as endocrine disruptors: a technical review of the observational and clinical data. *Crit Rev Food Sci Nutr*. 2022;62:5824–85.
- Felix FB, Vago JP, Beltrami VA, Araújo JMD, Grespan R, Teixeira MM, et al. Biochanin A as a modulator of the inflammatory response: an updated overview and therapeutic potential. *Pharmacol Res*. 2022;180:106246.
- Roland WSU, Vincken J-P, Gouka RJ, van Buren L, Gruppen H, Smit G. Soy isoflavones and other Isoflavonoids activate the human bitter taste receptors hTAS2R14 and hTAS2R39. *J Agric Food Chem*. 2011;59:11764–71.
- Xu S, Yu S, Dong D, Lee LTO. G protein-coupled estrogen receptor: a potential therapeutic target in Cancer. *Front Endocrinol (Lausanne)*. 2019;10:725.
- Luongo FP, Passaponti S, Haxhiu A, Raeispour M, Belmonte G, Governini L, et al. Bitter Taste Receptors and endocrine disruptors: Cellular and

- Molecular insights from an in vitro model of human granulosa cells. *Int J Mol Sci.* 2022;23:15540.
13. Lu P, Zhang C-H, Lifshitz LM, ZhuGe R. Extraoral bitter taste receptors in health and disease. *J Gen Physiol.* 2017;149:181–97.
 14. Kamila T, Agnieszka K. An update on extra-oral bitter taste receptors. *J Transl Med.* 2021;19:440.
 15. Talmon M, Pollastro F, Fresu LG. The Complex Journey of the calcium regulation downstream of TAS2R activation. *Cells.* 2022;11:3638.
 16. Gentiluomo M, Crifasi L, Luddi A, Locci D, Barale R, Piomboni P, et al. Taste receptor polymorphisms and male infertility. *Hum Reprod.* 2017;32:2324–31.
 17. Yu X, Zhen Y, Fang T, Zhang J, Xu Y, Wu F et al. Advances in the study of the role of extraoral bitter taste receptors. [cited 2024 Aug 6]; Available from: <https://www.authorea.com/users/619381/articles/643927-advances-in-the-study-of-the-role-of-extraoral-bitter-taste-receptors?commit=6481cfaf41594d8ceb4b28bf9e28fde32421d9a2>.
 18. Wu S, Xue P, Grayson N, Bland JS, Wolfe A. Bitter Taste Receptor Ligand improves metabolic and Reproductive functions in a murine model of PCOS. *Endocrinology.* 2019;160:143–55.
 19. Semplici B, Luongo FP, Passaponti S, Landi C, Governini L, Morgante G, et al. Bitter taste receptors expression in human granulosa and Cumulus cells: New perspectives in female fertility. *Cells.* 2021;10:3127.
 20. Jiang J, Liu S, Qi L, Wei Q, Shi F. Activation of ovarian taste receptors inhibits Progesterone Production potentially via NO/cGMP and apoptotic signaling. *Endocrinology.* 2021;162:bqaa240.
 21. Anuranjana PV, Beegum F, George KPD, Viswanatha KT, Nayak GL. Mechanisms behind the pharmacological application of Biochanin-A: a review. *F1000Res.* 2023;12:107.
 22. Wölfle U, Elsholz FA, Kersten A, Haarhaus B, Schumacher U, Schempp CM. Expression and functional activity of the human bitter taste receptor TAS2R38 in human placental tissues and JEG-3 cells. *Molecules.* 2016;21:306.
 23. Rhyu M-R, Kim Y, Misaka T. Suppression of hTAS2R16 Signaling by Umami substances. *Int J Mol Sci.* 2020;21:7045.
 24. Zhang Y, Wang X, Li X, Peng S, Wang S, Huang CZ, et al. Identification of a specific agonist of human TAS2R14 from Radix Bupleuri through virtual screening, functional evaluation and binding studies. *Sci Rep.* 2017;7:12174.
 25. Suess B, Brockhoff A, Meyerhof W, Hofmann T. The odorant (R)-Citronellal attenuates caffeine bitterness by inhibiting the bitter receptors TAS2R43 and TAS2R46. *J Agric Food Chem.* 2018;66:2301–11.
 26. Luddi A, Gori M, Marrocco C, Capaldo A, Pavone V, Bianchi L, et al. Matrix metalloproteinases and their inhibitors in human cumulus and granulosa cells as biomarkers for oocyte quality estimation. *Fertil Steril.* 2018;109:930–e9393.
 27. Luddi A, Marrocco C, Governini L, Semplici B, Pavone V, Luisi S et al. Expression of Matrix metalloproteinases and their inhibitors in Endometrium: high levels in endometriotic lesions. *Int J Mol Sci.* 2020;21:2840.
 28. Luongo FP, Dragoni F, Boccuto A, Paccagnini E, Gentile M, Canosi T, et al. SARS-CoV-2 infection of human ovarian cells: a potential negative impact on female fertility. *Cells.* 2022;11:1431.
 29. Puggioni E, Governini L, Gori M, Belmonte G, Piomboni P, Costantino-Ceccarini E, et al. Morphological and molecular characterisation of twitcher mouse spermatogenesis: an update. *Reprod Fertil Dev.* 2016;28:1258.
 30. Greene TA, Alarcon S, Thomas A, Berdougou E, Doranz BJ, Breslin PAS, et al. Probenecid inhibits the human bitter taste receptor TAS2R16 and suppresses bitter perception of salicin. *PLoS ONE.* 2011;6:e20123.
 31. Dewi DA, Abayasekara DRE, Wheeler-Jones CPD. Requirement for ERK1/2 activation in the regulation of progesterone production in human granulosa-lutein cells is stimulus specific. *Endocrinology.* 2002;143:877–88.
 32. Baddela VS, Michaelis M, Tao X, Koczan D, Vanselow J. ERK1/2-SOX9/FOXL2 axis regulates ovarian steroidogenesis and favors the follicular–luteal transition. *Life Sci Alliance.* 2023;6:e202302100.
 33. Jeruzal-Świątecka J, Fendler W, Pietruszewska W. Clinical role of Extraoral bitter taste receptors. *Int J Mol Sci.* 2020;21:5156.
 34. Shin JW, Park SH, Kang YG, Wu Y, Choi HJ, Shin J-W. Changes, and the Relevance Thereof, in mitochondrial morphology during differentiation into endothelial cells. *PLoS ONE.* 2016;11:e0161015.
 35. Glancy B, Kim Y, Katti P, Willingham TB. The functional impact of mitochondrial structure across subcellular scales. *Front Physiol.* 2020;11:541040.
 36. Park J, Lee J, Choi C. Mitochondrial network determines intracellular ROS dynamics and sensitivity to oxidative stress through switching inter-mitochondrial messengers. *PLoS ONE.* 2011;6:e23211.
 37. Miller WL. Steroidogenic enzymes. *Endocr Dev.* 2008;13:1–18.
 38. Kaplanski O, Shemesh M, Berman A. Effects of phyto-oestrogens on progesterone synthesis by isolated bovine granulosa cells. *J Endocrinol.* 1981;89:343–8.
 39. Seger R, Hanoch T, Rosenberg R, Dantes A, Merz WE, Jerome F, Strauss III, et al. The ERK Signaling Cascade inhibits Gonadotropin-stimulated steroidogenesis. *J Biotechnol Biomed.* 2023;6:1.
 40. Duarte A, Castillo AF, Podestá EJ, Poderoso C. Mitochondrial Fusion and ERK Activity Regulate Steroidogenic Acute Regulatory Protein Localization in Mitochondria. *PLoS ONE.* 2014;9:e100387.
 41. Jefferi NES, Shamhari A, Afifah, Hamid ZA, Budin SB, Zulkifly AMZ, Roslan FN, et al. Knowledge gap in understanding the Steroidogenic Acute Regulatory Protein Regulation in Steroidogenesis following exposure to Bisphenol A and its analogues. *Biomedicines.* 2022;10:1281.
 42. Yu X-H, Chen J-J, Deng W-Y, Xu X-D, Liu Q-X, Shi M-W, et al. Biochanin A mitigates atherosclerosis by inhibiting lipid Accumulation and Inflammatory Response. *Oxid Med Cell Longev.* 2020;2020:8965047.
 43. Talbott HA, Plewes MR, Krause C, Hou X, Zhang P, Rizzo WB, et al. Formation and characterization of lipid droplets of the bovine corpus luteum. *Sci Rep.* 2020;10:11287.
 44. Pu Q, Guo K, Lin P, Wang Z, Qin S, Gao P, et al. Bitter receptor TAS2R138 facilitates lipid droplet degradation in neutrophils during *Pseudomonas aeruginosa* infection. *Signal Transduct Target Ther.* 2021;6:210.
 45. Rasbach KA, Schnellmann RG. Isoflavones promote mitochondrial Biogenesis. *J Pharmacol Exp Ther.* 2008;325:536–43.
 46. Bikas A, Jensen K, Patel A, Costello J, Reynolds SM, Mendonca-Torres MC, et al. Cytochrome C oxidase subunit 4 (COX4): a potential therapeutic target for the treatment of medullary thyroid Cancer. *Cancers.* 2020;12:2548.
 47. Kaseder M, Schmid N, Eubler K, Goetz K, Müller-Taubenberger A, Dissen GA, et al. Evidence of a role for cAMP in mitochondrial regulation in ovarian granulosa cells. *Mol Hum Reprod.* 2022;28:gaac030.
 48. Oliva CR, Markert T, Gillespie GY, Griguer CE. Nuclear-encoded cytochrome c oxidase subunit 4 regulates BMI1 expression and determines proliferative capacity of high-grade gliomas. *Oncotarget.* 2015;6:4330–44.
 49. Westermann B. Bioenergetic role of mitochondrial fusion and fission. *Biochim Biophys Acta.* 2012;1817:1833–8.
 50. Youle RJ, van der Bliek AM. Mitochondrial fission, fusion, and stress. *Science.* 2012;337:1062–5.
 51. Liesa M, Shirihai OS. Mitochondrial dynamics in the regulation of nutrient utilization and energy expenditure. *Cell Metab.* 2013;17:491–506.
 52. Feng Z-J, Lai W-F. Chemical and Biological properties of Biochanin A and its Pharmaceutical Applications. *Pharmaceutics.* 2023;15:1105.
 53. Yu C, Zhang P, Lou L, Wang Y. Perspectives Regarding the Role of Biochanin A in Humans. *Front Pharmacol.* 2019 [cited 2024 Nov 18];10. Available from: <https://www.frontiersin.org/journals/pharmacology/articles/10.3389/fphar.2019.00793/full>.
 54. Moon YJ, Sagawa K, Frederick K, Zhang S, Morris ME. Pharmacokinetics and bioavailability of the isoflavone biochanin A in rats. *AAPS J.* 2006;8:51.
 55. Sahoo DK, Heilmann RM, Paital B, Patel A, Yadav VK, Wong D et al. Oxidative stress, hormones, and effects of natural antioxidants on intestinal inflammation in inflammatory bowel disease. *Front Endocrinol.* 2023 [cited 2024 Nov 18];14. Available from: <https://www.frontiersin.org/journals/endocrinology/articles/10.3389/fendo.2023.1217165/full>.
 56. Salla M, Karaki N, El Kaderi B, Ayoub AJ, Younes S, Abou Chahla MN, et al. Enhancing the bioavailability of Resveratrol: combine it, Derivatize it. Or Encapsulate It? *Pharm.* 2024;16:569.

Publisher's Note

Springer Nature remains neutral with regard to jurisdictional claims in published maps and institutional affiliations.